Topological edge breathers in a nonlinear Su-Schrieffer-Heeger lattice

Magnus Johansson

Department of Physics, Chemistry and Biology (IFM), Linköping University, SE-581 83, Linköping, Sweden

ARTICLE INFO

ABSTRACT

We show the existence of breathing edge modes in the Su-Schrieffer-Heeger model with cubic (Kerr) on-site nonlinearity, bifurcating from stationary edge solitons with propagation constant inside the topological gap of the linear model. These edge breathers are exact solutions to the nonlinear equations of motion, with time-periodic intensity oscillations and tails exponentially decaying from the edge. They bifurcate from two localized internal eigenmodes of the stationary edge soliton, having eigenfrequencies inside the topological gap and all higher harmonics above the linear spectrum. Numerical Floquet analysis for solutions obtained from a Newton scheme shows that edge breathers may be linearly stable even in regimes of large-amplitude oscillations, mainly manifested as time-periodic power exchange between the edge site and its next-nearest neighbor.

There has been a large recent interest in the study of nonlinear effects in lattices with topologically induced gaps in their linear spectra, particularly within nonlinear optics which has led to the emerging field of nonlinear topological photonics (see reviews [1,2]), but also more generally for, e.g., mechanical or electrical lattices (see, e.g., recent works [3,4] and references therein). To elucidate the most fundamental effects arising from the simultaneous presence of topology and nonlinearity, much attention has been directed to nonlinear generalizations of the one-dimensional Su-Schrieffer-Heeger (SSH) lattice [5]. With a suitably chosen on-site nonlinearity (typically cubic Kerr or saturable), this model has an immediate realization using waveguide arrays with alternating spacings, and in this context properties of nonlinear localized modes with propagation constant inside the topological gap were studied earlier in some detail, theoretically as well as experimentally [6–9]. If the dimerized SSH chain is terminated by a half-dimer edge there is an exponentially localized mid-gap edge state in the linear limit, which continues with nonlinearity into an edge soliton whose propagation constant remains within the topological gap for sufficiently weak nonlinearity ("nonlinear Shockley-like states" as discussed in [7]). A more recent work showed that in the continuum limit, stationary bulk and edge gap solitons are obtained from the same family of solutions to the nonlinear Dirac equation [10].

The linear stability of discrete bulk gap solitons was analyzed in detail for the SSH model with Kerr nonlinearity in [6] (see also [9] for the saturable case), and more recently for topological edge

solitons in [11]. If signs are chosen such that the bulk gap soliton bifurcates from the lower band, it remains stable in the lower half of the gap but destabilizes through an oscillatory instability in the upper half if the ratio between the coupling constants is not too far from unity [6]. A similar scenario, with oscillatory instability above a critical coupling ratio, was later found for the edge soliton [11], which only exists in the upper half of the gap (the similarity is clearly seen by comparing the stability diagrams obtained in Fig. 5(a) of Ref. [6] and in Fig. 4 of Ref. [11]). In both cases, the instabilities are caused by resonances either between a localized internal soliton oscillation mode and extended modes from the continuous spectrum, or between two localized modes originating from the two different sub-bands [6,11]. Similar instability mechanisms have been described also for mechanical analogs of the SSH model [3,12,13]. The long-term dynamics arising from the unstable edge modes in mechanical lattices has been seen to, after an initial oscillatory behavior, typically lead to a chaotic spreading into the lattice, while leaving only a small-amplitude linear edge mode at the edge [3,12]. On the other hand, for the Kerr nonlinear case the example shown in Fig. 5 of Ref. [11] (although for a considerably shorter time-scale) indicated the transition into a stable *nonlinear* edge state with smaller power, together with small-amplitude, possibly decaying internal-mode oscillations. The excitation of a nonlinear topological edge mode with long-lived internal oscillations has also been illustrated in [14] (see Fig. 2(a4) in this paper) using a single-site initial condition for the Kerr nonlinear SSH model.

With the above background, it is relevant to ask whether the nonlinear SSH model may support more general, possibly stable, solutions localized at the half-dimer edge, in addition to the sta-

E-mail address: magjo23@liu.se.

tionary topological edge modes. As we will show here, the answer is in the affirmative. We will show that also *breathing* edge modes, with time-periodic intensity oscillations, appear as *exact* solutions to the Kerr nonlinear SSH model in certain parameter regimes. They appear as continuous solution families, extending the linear internal modes of the stationary edge solitons into the fully nonlinear regime. It is important here to realize the distinction between the excitation of a linear internal oscillation mode, which appears commonly for solitons in non-integrable system and in general decays with time due to resonance with extended eigenmodes, and the exact breathing solitons obtained here. As is known [15], the linear eigenmodes can be continued into nonlinear exact solutions only in cases where all their higher harmonics are outside the continuous spectrum. As we will see here, this enforces certain restrictions on the parameter values.

Note that for bulk gap modes, the existence of exact breathing solitons was pointed out already in [6], due to the existence of an internal mode with frequency above the continuous spectrum (and consequently also having all higher harmonics above the spectrum). This feature is analogous to the (non-topological) case with alternating linear on-site energies [16] (modeling, e.g., a waveguide array with constant spacings but alternating widths), for which exact breathing gap solitons were explicitly calculated numerically in [17] using a Newton scheme originally developed in [18]. However, as we will see below, the situation is somewhat more intricate for the topological edge modes since the internal mode frequencies are inside the gap, and thus one must assure that non-resonance conditions are fulfilled to avoid second-harmonic resonances with the upper branch of the continuous spectrum.

We consider the following form of the SSH model with Kerr onsite nonlinearity:

$$i\dot{\psi}_n + C\left\{\left[1 + (-1)^n\delta\right]\psi_{n-1} + \left[1 - (-1)^n\delta\right]\psi_{n+1}\right\} + |\psi_n|^2\psi_n = 0, \tag{1}$$

with $1 \leq n \leq N$ and boundary conditions $\psi_0 = \psi_{N+1} = 0$. With these conventions and $0 < \delta < 1$, the lattice is terminated with a full dimer at the left edge, and a half dimer at the right if N is odd (as the coupling between sites 1 and 2 is strong while that between sites $N - 1$ and N is weak for odd N). Thus, the topological edge state exists only at the right edge. Furthermore, we may rescale to put the average coupling constant $C = 1$ (this is done in all numerical results reported below). We will refer to the overdot as a derivative with respect time, although for a waveguide array it would correspond to a longitudinal spatial coordinate. There are two conserved quantities associated with Eq. (1), power (norm) $P = \sum_n |\psi_n|^2$, and Hamiltonian which may be defined as $H = \sum_n \left\{-C\left[1 - (-1)^n\delta\right]\left(\psi_n\psi_{n+1}^* + \psi_n^*\psi_{n+1}\right) - \frac{1}{2}|\psi_n|^4\right\}$ (with a sign convention such that $i\dot{\psi}_n = \partial H/\partial\psi_n^*$).

Expressing a stationary solution to Eq. (1) as $\psi_n(t) = \phi_n^{(\Lambda)}e^{i\Lambda t}$, with $\phi_n^{(\Lambda)}$ time-independent, the two bands of the linear spectrum have frequencies in the intervals $[-2C, -2C\delta]$ and $[2C\delta, 2C]$, and the topological edge soliton exists in the upper half of the gap, $\Lambda \in [0, 2C\delta]$ (with the sign of the frequency Λ chosen to have $\Lambda > 0$ for $C > 0$). Its linear stability is determined in the standard way [6,11,16] by expressing a perturbed stationary solution as $\psi_n(t) = [\phi_n^{(\Lambda)} + \epsilon_n(t)]e^{i\Lambda t}$, with $\epsilon_n(t) = \frac{1}{2}(\xi_n + \eta_n)e^{-i\omega_l t} + \frac{1}{2}(\xi_n^* - \eta_n^*)e^{i\omega_l^* t}$. Linearizing and solving the resulting eigenvalue problem yields the small-amplitude oscillation frequencies ω_l, with linear stability requiring all ω_l to be real. The overall stability properties were illustrated in Figs. 3-4 of Ref. [11], from which it was concluded that the edge soliton is stable for all Λ if the ratio of the coupling constants $t \equiv \frac{1-\delta}{1+\delta} < t_c \approx 0.35$ (i.e., if $\delta \gtrsim 0.48$), while intervals of oscillatory instability appear for $t > t_c$ ($\delta \lesssim 0.48$). Below
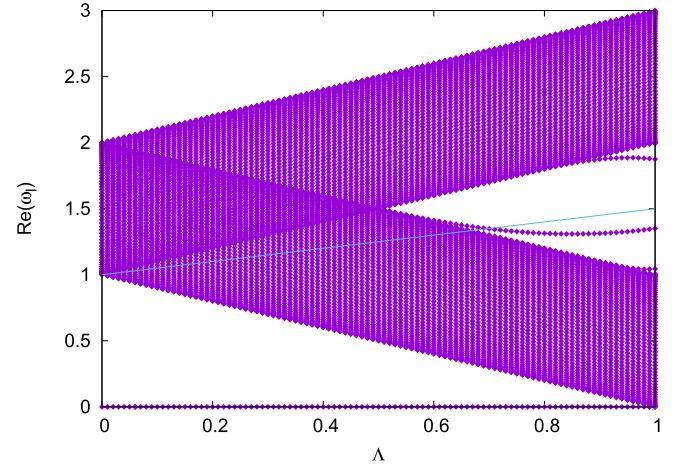

Fig. 1. Real parts of linear eigenfrequencies ω_l versus propagation constant Λ for stationary edge solitons when $\delta = 0.5$ ($N = 121$ sites). The spectrum is symmetric around $\omega_l = 0$ so only positive eigenfrequencies are shown. The thin blue line indicates the condition for avoiding higher-harmonic resonances: modes with eigenfrequencies above the line have all harmonics above the upper band. (For interpretation of the colors in the figure(s), the reader is referred to the web version of this article.)

we discuss some additional features which are essential to understand the conditions for having breathing edge modes as exact solutions.

For illustration, we plot in Fig. 1 the (positive) real part of the linear eigenfrequencies as a function of the propagation constant for the family of stable stationary edge solitons when $\delta = 0.5$. The continuous spectrum (extended eigenmodes) is the same as for the bulk solitons discussed in [6] (cf. Fig. 4 of [6]): it consists of two bands $[2C\delta + \Lambda, 2C + \Lambda]$ and $[2C\delta - \Lambda, 2C - \Lambda]$, which overlap if $\Lambda < C(1 - \delta)$. Since $\Lambda < 2C\delta$ for any gap mode, a regime with non-overlapping bands exists only when $\delta > 1/3$ (i.e., for coupling ratio $t < 1/2$).

In addition, as seen in Fig. 1, two localized internal modes appear in the gap, bifurcating from the upper and lower subbands, respectively (these are the modes that will resonate and cause the regimes of oscillatory instabilities when $\delta \lesssim 0.48$ [11]). The condition for having all higher harmonics of these modes above the continuous spectrum then becomes $\omega_l > \frac{\Lambda}{2} + C$ (thin blue line in Fig. 1), which is easily seen to be always fulfilled for any internal mode in the gap sufficiently close to the upper band. Furthermore, as seen from Fig. 1, there may be a regime where also the mode originating from the lower band has all its harmonics above the upper band ($0.55 \lesssim \Lambda/C \lesssim 0.70$ for $\delta = 0.5$). From a more systematic investigation, we may conclude that stable topological edge solitons having internal modes with all higher harmonics outside the continuous spectrum exist for all $\delta \gtrsim 0.42$: the mode originating from the upper band always exists in a regime of larger Λ ($0.85 \lesssim \Lambda < 1.0$ in Fig. 1), while that from the lower band has some regime in Λ fulfilling the non-resonance condition if $0.42 \lesssim \delta \lesssim 0.57$. For $\delta \lesssim 0.41$ (coupling ratio $t \gtrsim 0.42$), no localized internal modes exist for stable edge solitons. We may remark that simulations in Fig. 5 of [11], showing decaying oscillations, corresponded to a coupling ratio with no stable internal mode ($t = 0.43$), while those of Fig. 2(a4) in [14], showing apparently persistent oscillations, corresponded to a case with possibility for excitation of both modes in non-resonant regimes ($\delta = 0.5$).

We now turn to the explicit numerical calculations of the families of exact, nonlinearly breathing, edge solitons arising from the non-resonant linear internal eigenmodes. The numerical Newton method is the same as in [17] (see also [18], to which we refer for details). Transforming to a rotating frame, $\psi_n(t) = \phi_n(t)e^{i\omega_0 t}$, breathing solitons are sought as solutions which, for given ω_0, are

time-periodic in ϕ_n with frequency ω_b, $\phi_n(t + 2\pi/\omega_b) = \phi_n(t)$. As we are looking for nonlinear continuations of linear eigenmodes, with frequency ω_l, of stationary edge modes with frequency Λ, we use trial solutions obtained by adding small-amplitude linear eigenvectors to the stationary solution, and search for numerically exact solutions ($||\phi_n(t+2\pi/\omega_b)-\phi_n(t)|| < 10^{-12}$) with ω_0 close to Λ and ω_b close to ω_l. After convergence, linear stability is obtained from a standard numerical Floquet analysis [17,18], with linear stability being equivalent to having all eigenvalues on the unit circle.

As a specific example, we here show families of exact edge breathers obtained with $\delta = 0.43$. In this case, a stable stationary edge soliton in the gap ($\Lambda/C < 0.86$) has a non-resonant internal mode originating from the upper band when $\Lambda/C \gtrsim 0.73$, and a non-resonant mode from the lower band when $\Lambda/C \gtrsim 0.62$. Fig. 2 illustrates the family of breathing solutions continued from the lower-branch internal mode at constant $\omega_0 = 0.67$. As is seen from the upper figure, the oscillations mainly result from significant power exchanges between the edge site and its next-nearest neighbor. Note also that the oscillations for the example shown are sufficiently large so that the minimum $|\psi|$ at the edge site becomes slightly smaller than the maximum $|\psi|$ at the next-nearest neighbor (i.e., the solution attains a 'pulson' character with the terminology of [17]). Concerning the phase of ψ_n, these two (next-nearest neighboring) sites are seen to retain a phase difference close to π during the oscillations, and likewise the wave vector for the exponentially decaying tail remains close to $\pi/2$ as for the stationary edge mode in the gap.

From the central part of Fig. 2 we note that the continuation versus breathing frequency ω_b from the linear eigenmode at $\omega_b = \omega_l$ in this case becomes non-monotonous: starting at $\omega_l \approx 1.451$ the breathing frequency first decreases with increasing oscillation amplitude, reaches a minimum around $\omega_b \approx 1.445$ and then increases until it meets the extended linear eigenmode at the lower edge of the upper linear band at $\omega_b = 1.53$. The stability analysis illustrated in the bottom of Fig. 2 shows that while the breather is essentially linearly stable in regimes of small and moderate oscillation amplitudes, it destabilizes through a single real Floquet eigenvalue becoming larger than one when oscillations become too large. Also for smaller amplitudes some Floquet eigenvalues may be located slightly outside the unit circle, but these correspond to resonances between extended eigenmodes which may cause weak instabilities for smaller lattice sizes, disappearing in the limit of a semi-infinite chain [19] ("bulk-bulk" instabilities in the terminology of [12,13]). We also checked with direct numerical integration that the solution shown in the upper Fig. 2 for the smaller system of 121 sites indeed destabilizes after long-time integration, but that, for a fixed perturbation strength, the time until destabilization increases rapidly with increasing system size. However, for these particular parameter values the breather is still quite fragile with respect to larger perturbations, since it is close to the instability threshold. Breathers with smaller oscillations tend to be generally more stable.

When moving into a regime of slightly stronger nonlinearity ($0.73 \lesssim \Lambda/C < 0.86$ when $\delta = 0.43$), there may be two simultaneously existing distinct families of stable breathers, arising from continuation of the two different linear eigenmodes of the stationary edge soliton. In order to make a proper comparison between these families we perform a continuation at constant power P, allowing the harmonic frequency ω_0 to be a free parameter (cf. [17,18,20]), since P and not ω_0 is a conserved quantity of Eq. (1). Fig. 3 illustrates the continuation of both families at $P = 1.8$, corresponding to a stationary frequency $\Lambda \approx 0.8274$. From the shown dependence of the Hamiltonian vs. breathing frequency, some features should be especially noted:
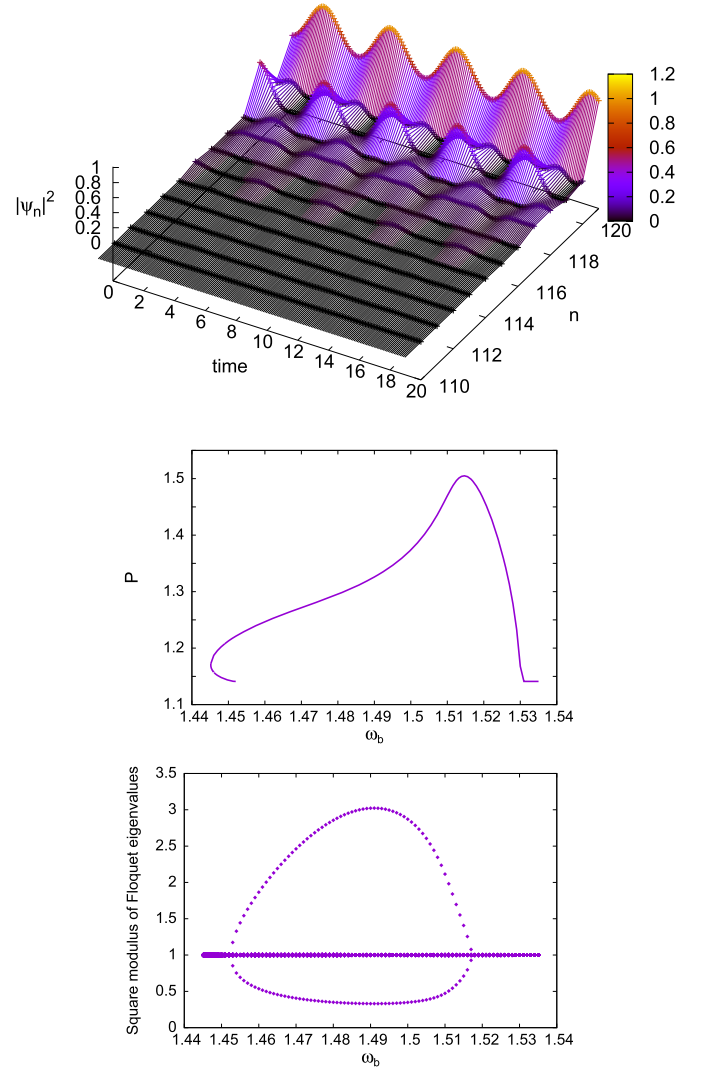

Fig. 2. Top: Short-time evolution of a linearly stable breathing edge soliton. Parameter values $\delta = 0.43$, $\omega_0 = 0.67$, $\omega_b = 1.45$, and $N = 121$ sites (only a small part around the right edge is shown). Middle: Power vs. ω_b for the corresponding full family of breathers at constant ω_0. The solution shown belongs to the upper branch at $\omega_b = 1.45$. The family bifurcates from the stationary solution at $\Lambda = \omega_0$ having $P \approx 1.141$. Bottom: Square modulus of Floquet eigenvalues vs. ω_b for the same family.

- The bifurcations from the stationary edge soliton appear as before at the linear eigenfrequencies ω_l; $\omega_b \approx 1.600$ for the mode originating from the upper band (thick purple line) and $\omega_b \approx 1.492$ for that from the lower (thin green line), respectively.
- The continuation into the regime of slightly nonlinear oscillations increases (decreases) as well the breathing frequency as the Hamiltonian for the mode from the upper (lower) band. The latter is related to the Krein signature of the corresponding linear eigenmode which gives the sign of the Hamiltonian energy carried by the mode (cf., e.g., [20] and references therein); with the sign conventions used here, modes from the upper (lower) band have positive (negative) Krein signature.
- The continuation vs. ω_b is now monotonous in the whole range of existence for the family from the lower band, while that from the upper band has three turning points.
- For both families the continuation shows a sharp increase in H at some critical smaller ω_b; this corresponds to a second-harmonic resonance with a mode from the upper edge of the upper band when $\omega_b \approx \omega_0/2 + C$. The continuation can be per-
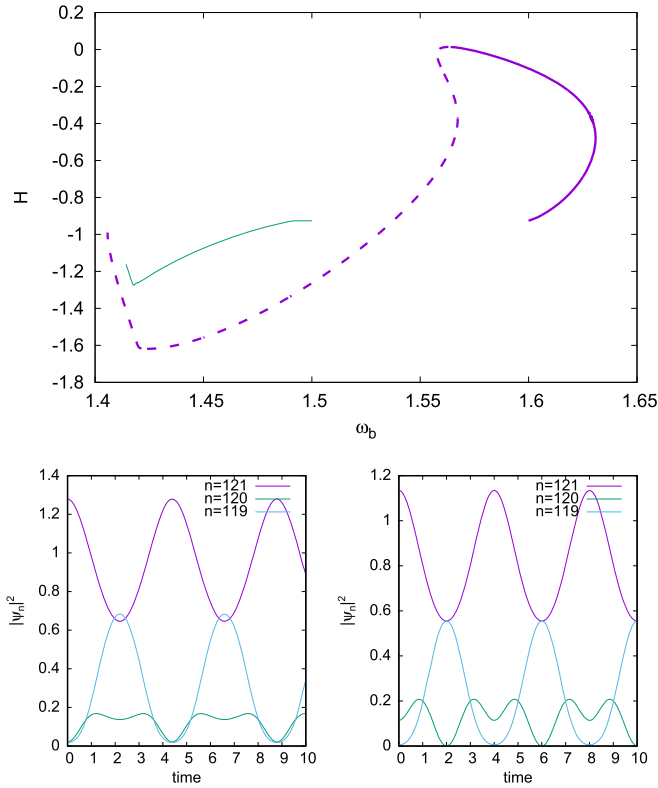
Fig. 3. Upper: Hamiltonian vs. ω_b at constant power $P = 1.8$ for the two different families of breathers continued from the two localized internal modes of the stationary edge soliton for $\delta = 0.43$. Dashed lines indicate regimes of instability. $N = 121$ sites. The continuations were interrupted for smaller ω_b as solutions became non-localized. Lower: Dynamics at the edge site and its two nearest neighbors for linearly stable exact breathers belonging to each of the two families. Left: lower-band family at $\omega_b = 1.43$, $\omega_0 \approx 0.838$. Right: upper-band family at $\omega_b = 1.57$, $\omega_0 \approx 0.746$.

formed towards smaller ω_b but the solution will no longer be exponentially localized due to the second-harmonic extended tail.

- From the Floquet analysis (not shown) the family from the lower band is now found to be linearly stable (except for finite-size instabilities as above) in its full range of existence as a localized breather, while that from the upper band destabilizes for $\omega_b \lesssim 1.563$. The instability threshold appears at the point where $dH/d\omega_b = 0$, which appears to be a general sufficient condition for a stability change through a collision of Floquet eigenvalues at +1 when continuation is performed at constant P [20] (this condition would not be valid for continuations at constant ω_0).

The main qualitiative differences between the oscillation patterns in the two families are illustrated in the lower parts of Fig. 3. While in both cases the main oscillation is the power exchange between the edge site and its next-nearest neighbor, the smaller oscillations at the nearest neighbor differ. For the lower-band family the two sites in the neighboring dimer mainly oscillate in phase, while they oscillate largely out-of phase for the upper-band family. As a result, for the lower-band family the neighboring dimer may become almost depleted at the instants when the edge site peaks, while for the upper-band family the nearest-neighbor site then has a considerable amplitude which instead almost vanishes when the edge site has its minimum.

In conclusion, we showed that two families of topological edge breathers may appear as exact and linearly stable localized solutions to the nonlinear SSH model under certain parameter condi-

tions, and used numerical continuation methods for their explicit calculation. Generally, edge breathers would appear in any lattice supporting an edge soliton with localized internal modes having all higher harmonics outside the linear spectrum of extended modes, and whether such modes exist also for two-dimensional topological systems may be an interesting direction for future research. There are already many experiments confirming the existence of edge and interface solitons (topological as well as non-topological) in SSH-related systems (e.g., [7,8,21–23]), and it would be highly interesting to see whether also these edge breathers could be generated in realistic setups. The fact that long-lived oscillations may be generated from a simple single-site initial condition [14] may indicate that they could appear experimentally from a single-waveguide excitation in the relevant parameter regime; however whether these oscillations indeed correspond to excitation of exact breathers needs to be more carefully investigated.

A final remark concerning the system size may be relevant. Since our main aim here was to describe exponentially localized edge modes in an ideally semi-infinite system, we considered large system sizes in order to have a negligible influence from the opposite edge. For convenience we chose an odd number of sites with $\delta > 0$ and the topological edge mode located at the right edge, but we could equally well have chosen an even number of sites and $\delta < 0$ to have a fully topologically nontrivial SSH chain with two topological edge modes. The only visible effect on the results reported here would be an additional midgap mode in the linearized spectrum of Fig. 1, corresponding to the linear edge mode at the opposite edge. However, for smaller chains in the topologically nontrivial regime the two edge modes will hybridize, leading to power oscillations between the edges in the linear chain which may survive also in presence of Kerr nonlinearity [24]. The time scale for such oscillations would however be extremely large for the system sizes considered here.

Discussions with Aleksandra Maluckov, Milutin Stepić and Rodrigo Vicencio are gratefully acknowledged.

CRediT authorship contribution statement

Magnus Johansson: Writing – review & editing, Writing – original draft, Visualization, Validation, Software, Resources, Project administration, Methodology, Investigation, Formal analysis, Data curation, Conceptualization.

Declaration of competing interest

The authors declare that they have no known competing financial interests or personal relationships that could have appeared to influence the work reported in this paper.

Data availability

Data will be made available on request.

References

[1] D. Smirnova, D. Leykam, Y. Chong, Y. Kivshar, Nonlinear topological photonics, Appl. Phys. Rev. 7 (2020) 021306.

[2] M.J. Ablowitz, J.T. Cole, Nonlinear optical waveguide lattices: asymptotic analysis, solitons, and topological insulators, Physica D 440 (2022) 133440.

[3] B. Many Manda, R. Chaunsali, G. Teocharis, Ch. Skokos, Nonlinear topological edge states: from dynamic delocalization to thermalization, Phys. Rev. B 105 (2022) 104308.

[4] D. Zhou, D.Z. Rocklin, M. Leamy, Y. Yao, Topological invariant and anomalous edge modes of strongly nonlinear systems, Nat. Commun. 13 (2022) 3379.

[5] W.P. Su, J.R. Schrieffer, A.J. Heeger, Solitons in polyacetylene, Phys. Rev. Lett. 42 (1979) 1698.

[6] R.A. Vicencio, M. Johansson, Discrete gap solitons in waveguide arrays with alternating spacings, Phys. Rev. A 79 (2009) 065801.

[7] N. Malkova, I. Hromada, X. Wang, G. Bryant, Z. Chen, Transition between Tamm-like and Shockley-like surface states in optically induced photonic superlattices, Phys. Rev. A 80 (2009) 043806.

[8] A. Kanshu, C.E. Rüter, D. Kip, V. Shandarov, P.P. Beličev, I. Ilić, M. Stepić, Observation of discrete gap solitons in one-dimensional waveguide arrays with alternating spacings and saturable defocusing nonlinearity, Opt. Lett. 37 (2012) 1253.

[9] P.P. Beličev, I. Ilić, A. Maluckov, M. Stepić, A. Kanshu, C.E. Rüter, D. Kip, Dynamics of gap solitons in one-dimensional binary lattices with saturable defocusing nonlinearity and alternating spacing, Phys. Rev. A 86 (2012) 033835.

[10] D.A. Smirnova, L.A. Smirnov, D. Leykam, Y.S. Kivshar, Topological edge states and gap solitons in the nonlinear Dirac model, Laser Photonics Rev. 13 (2019) 1900223.

[11] Y.-P. Ma, H. Susanto, Topological edge solitons and their stability in a nonlinear Su-Schrieffer-Heeger model, Phys. Rev. E 104 (2021) 054206.

[12] R. Chaunsali, H. Xu, J. Yang, P.G. Kevrekidis, G. Teocharis, Stability of topological edge states under strong nonlinear effects, Phys. Rev. B 103 (2021) 024106.

[13] J.R. Tempelman, K.H. Matlack, A.F. Vakakis, Topological protection in a strongly nonlinear interface lattice, Phys. Rev. B 104 (2021) 174306.

[14] M. Ezawa, Nonlinearity-induced transition in the nonlinear Su-Schrieffer-Heeger model and a nonlinear higher-order topological system, Phys. Rev. B 104 (2021) 235420.

[15] P.G. Kevrekidis, M.I. Weinstein, Breathers on a background: periodic and quasiperiodic solutions of extended discrete nonlinear wave systems, Math. Comput. Simul. 62 (2003) 65.

[16] A.V. Gorbach, M. Johansson, Gap and out-gap breathers in a binary modulated discrete nonlinear Schrödinger model, Eur. Phys. J. D 29 (2004) 77.

[17] M. Johansson, A.V. Gorbach, Quasiperiodic localized oscillating solutions in the discrete nonlinear Schrödinger equation with alternating on-site potential, Phys. Rev. E 70 (2004) 057604.

[18] M. Johansson, S. Aubry, Existence and stability of quasiperiodic breathers in the discrete nonlinear Schrödinger equation, Nonlinearity 10 (1997) 1151.

[19] J.L. Marín, S. Aubry, Finite size effects on instabilities of discrete breathers, Physica D 119 (1998) 163.

[20] M. Johansson, Hamiltonian Hopf bifurcations in the discrete nonlinear Schrödinger model: a 'new' type of self-trapping transition, J. Phys. A, Math. Gen. 37 (2004) 2201.

[21] S. Xia, D. Jukić, N. Wang, D. Smirnova, L. Smirnov, L. Tang, D. Song, A. Szameit, D. Leykam, J. Xu, Z. Chen, H. Buljan, Nontrivial coupling of light into a defect: the interplay of nonlinearity and topology, Light: Sci. Appl. 9 (2020) 147.

[22] M. Guo, S. Xia, N. Wang, D. Song, Z. Chen, J. Yang, Weakly nonlinear topological gap solitons in Su-Schrieffer-Heeger photonic lattices, Opt. Lett. 45 (2020) 6466.

[23] Y.V. Kartashov, A.A. Arkhipova, S.A. Zhuravitskii, N.N. Skryabin, I.V. Dyakonov, A.A. Kalinkin, S.P. Kulik, V.O. Kompanets, S.V. Chekalin, L. Torner, V.N. Zadkov, Observation of edge solitons in topological trimer arrays, Phys. Rev. Lett. 128 (2022) 093901.

[24] N.K. Efremidis, Topological photonic Su-Schrieffer-Heeger-type coupler, Phys. Rev. A 104 (2021) 053531.